

Search for the decay $K^+ \rightarrow \pi^+ \gamma \gamma$ in the π^+ momentum region $P > 213 \text{ MeV}/c$

E949 Collaboration

A.V. Artamonov^a, B. Bassalleck^b, B. Bhuyan^{c,1},
 E.W. Blackmore^d, D.A. Bryman^e, S. Chen^{d,2}, I-H. Chiang^c,
 I.-A. Christidi^f, P.S. Cooper^g, M.V. Diwan^c, J.S. Frank^c,
 T. Fujiwara^h, J. Hu^d, D.E. Jaffe^c, S. Kabeⁱ, S.H. Kettell^c,
 M.M. Khabibullin^j, A.N. Khotjantsev^j, P. Kitching^{k,3},
 M. Kobayashiⁱ, T.K. Komatsubaraⁱ, A. Konaka^d,
 A.P. Kozhevnikov^a, Yu.G. Kudenko^j, A. Kushnirenko^{g,4},
 L.G. Landsberg^a, B. Lewis^b, K.K. Li^c, L.S. Littenberg^c,
 J.A. Macdonald^{d,5}, J. Mildemberger^d, O.V. Mineev^j,
 M. Miyajima^l, K. Mizouchi^h, V.A. Mukhin^a, N. Muramatsu^m,
 T. Nakano^m, M. Nomachiⁿ, T. Nomura^h, T. Numao^d,
 V.F. Obraztsov^a, K. Omataⁱ, D.I. Patalakha^a, S.V. Petrenko^a,
 R. Poutissou^d, E.J. Ramberg^g, G. Redlinger^c, T. Satoⁱ,
 T. Sekiguchiⁱ, T. Shinkawa^o, R.C. Strand^c, S. Sugimotoⁱ,
 Y. Tamagawa^l, R. Tschirhart^g, T. Tsunemi^{i,6}, D.V. Vavilov^a,
 B. Viren^c, N.V. Yershov^j, Y. Yoshimuraⁱ, T. Yoshioka^{i,7}

^a*Institute for High Energy Physics, Protvino, Moscow Region, 142 280, Russia*

^b*Department of Physics and Astronomy, University of New Mexico, Albuquerque, NM 87131, USA*

^c*Brookhaven National Laboratory, Upton, NY 11973, USA*

^d*TRIUMF, 4004 Wesbrook Mall, Vancouver, British Columbia, Canada V6T 2A3*

^e*Department of Physics and Astronomy, University of British Columbia, Vancouver, British Columbia, Canada V6T 1Z1*

^f*Department of Physics and Astronomy, Stony Brook University, Stony Brook, NY 11794, USA*

^g*Fermi National Accelerator Laboratory, Batavia, IL 60510, USA*

^h*Department of Physics, Kyoto University, Sakyo-ku, Kyoto 606-8502, Japan*

ⁱ*High Energy Accelerator Research Organization (KEK), Oho, Tsukuba, Ibaraki 305-0801, Japan*

^j*Institute for Nuclear Research RAS, 60 October Revolution Pr. 7a, 117312
Moscow, Russia*

^k*Centre for Subatomic Research, University of Alberta, Edmonton, Canada T6G
2N5*

^l*Department of Applied Physics, Fukui University, 3-9-1 Bunkyo, Fukui, Fukui
910-8507, Japan*

^m*Research Center for Nuclear Physics, Osaka University, 10-1 Mihogaoka,
Ibaraki, Osaka 567-0047, Japan*

ⁿ*Laboratory of Nuclear Studies, Osaka University, 1-1 Machikaneyama, Toyonaka,
Osaka 560-0043, Japan*

^o*Department of Applied Physics, National Defense Academy, Yokosuka, Kanagawa
239-8686, Japan*

Abstract

We have searched for the $K^+ \rightarrow \pi^+ \gamma \gamma$ decay in the kinematic region with π^+ momentum close to the end point. No events were observed, and the 90% confidence-level upper limit on the partial branching ratio was obtained, $B(K^+ \rightarrow \pi^+ \gamma \gamma, P > 213 \text{ MeV}/c) < 8.3 \times 10^{-9}$ under the assumption of chiral perturbation theory including next-to-leading order “unitarity” corrections. The same data were used to determine an upper limit on the $K^+ \rightarrow \pi^+ \gamma$ branching ratio of 2.3×10^{-9} at the 90% confidence level.

Key words: kaon rare decay, chiral perturbation theory, unitarity corrections, noncommutative theories

PACS: 13.20.Eb, 12.39.Fe, 11.10.Nx

¹ Also at the Department of Physics and Astrophysics, University of Delhi, Delhi 110007, India. Present address: Department of Physics and Astronomy, University of Victoria, Victoria, British Columbia, Canada V8W 3P6.

² Present address: Department of Engineering Physics, Tsinghua University, Beijing 100084, P.R. China.

³ Present address: TRIUMF, Canada.

⁴ Present address: Institute for High Energy Physics, Protvino, Russia.

⁵ Deceased.

⁶ Present address: Research Center for Nuclear Physics, Osaka University, Japan.

⁷ Present address: International Center for Elementary Particle Physics, University of Tokyo, Tokyo 113-0033, Japan.

We report the results of a search for the rare decay $K^+ \rightarrow \pi^+\gamma\gamma$ in the π^+ momentum region $P > 213$ MeV/ c from the E949 experiment [1] at the Alternating Gradient Synchrotron (AGS) of Brookhaven National Laboratory. The first observation of the decay in the π^+ momentum region 100–180 MeV/ c was reported [2] by the E787 experiment at the AGS with a partial branching ratio of $B(K^+ \rightarrow \pi^+\gamma\gamma, 100 \text{ MeV}/c < P < 180 \text{ MeV}/c) = (6.0 \pm 1.5(\text{stat}) \pm 0.7(\text{syst})) \times 10^{-7}$. In the region $P > 215$ MeV/ c no $K^+ \rightarrow \pi^+\gamma\gamma$ decays were observed and, assuming a pure phase-space kinematic distribution, a 90% confidence-level (C.L.) upper limit of 5.0×10^{-7} was set on the total branching ratio [2]. This established that the $K^+ \rightarrow \pi^+\gamma\gamma$ background to the rare decay $K^+ \rightarrow \pi^+\nu\bar{\nu}$ [3] was negligible.

In an effective-field approach to low-energy hadronic interactions called chiral perturbation theory (ChPT) [4], there is no $O(p^2)$ (“tree-level”) contribution to $K^+ \rightarrow \pi^+\gamma\gamma$ or its neutral counterpart $K_L^0 \rightarrow \pi^0\gamma\gamma$; the leading contributions start at $O(p^4)$ [5]. For $K^+ \rightarrow \pi^+\gamma\gamma$, both the branching ratio and the π^+ spectrum shape at $O(p^4)$ are sensitive to the undetermined coupling-constant \hat{c} . There is no complete calculation at the next-to-leading order, $O(p^6)$. The dominant effects [6] are one-loop “unitarity” corrections, deduced from an empirical fit to the decay amplitude of $K^+ \rightarrow \pi^+\pi^+\pi^-$ and containing the same constant \hat{c} , and vector-meson exchange. In $K^+ \rightarrow \pi^+\gamma\gamma$ vector-meson exchange is expected to be negligible compared to unitarity corrections. The corrections result in a slightly different prediction for the π^+ spectrum (Fig. 1). Separate fits to the measured π^+ spectrum from [2] with and without the unitarity corrections yielded $\hat{c} = 1.8 \pm 0.6$ and $\hat{c} = 1.6 \pm 0.6$, respectively, but slightly preferred their inclusion. For $K_L^0 \rightarrow \pi^0\gamma\gamma$, the amplitude at $O(p^4)$ is determined without any undetermined coupling-constant, but the measured branching ratio, $(1.41 \pm 0.12) \times 10^{-6}$ [7], is twice as large as predicted at $O(p^4)$; the vector-meson contribution in the next-to-leading order calculation (sometimes parametrized by an effective coupling constant a_v) is considered to be important to this decay [8].

One of the consequences of the unitarity corrections to $K^+ \rightarrow \pi^+\gamma\gamma$ is a non-zero amplitude in the kinematic region close to the end point of $P = 227$ MeV/ c , where the two-photon invariant mass $m_{\gamma\gamma} = 0$ MeV/ c^2 , as shown in Fig. 1. The partial branching ratio $B(K^+ \rightarrow \pi^+\gamma\gamma, P > 213 \text{ MeV}/c)$, corresponding to $m_{\gamma\gamma} < 108 \text{ MeV}/c^2$, is predicted to be $6.10_{-0.12}^{+0.16} \times 10^{-9}$ for $\hat{c} = 1.8 \pm 0.6$ including unitarity corrections and $0.49_{-0.18}^{+0.23} \times 10^{-9}$ for $\hat{c} = 1.6 \pm 0.6$ without the corrections. Observation of the decay at a partial branching ratio larger than predicted would indicate the contribution of vector-meson exchange or other new dynamics to $K^+ \rightarrow \pi^+\gamma\gamma$. The kinematic region close to the end point in $K_L^0 \rightarrow \pi^0\gamma\gamma$ is known to be crucial to understand the CP-conserving component to the $K_L^0 \rightarrow \pi^0 e^+ e^-$ decay through the $K_L^0 \rightarrow \pi^0\gamma\gamma \rightarrow \pi^0 e^+ e^-$ amplitude, but experimental results on a_v in $K_L^0 \rightarrow \pi^0\gamma\gamma$ [9,10] are inconsistent (see Ref. [11,12] for theoretical discus-

sions).

E949 was designed primarily to measure the decay $K^+ \rightarrow \pi^+ \nu \bar{\nu}$ [13]. The AGS delivered kaons of 710 MeV/ c to the experiment at a rate of 12.8×10^6 per 2.2-s spill. Kaons, detected and identified by Čerenkov, tracking, and energy-loss counters, were slowed by BeO and active degraders, and came to rest and decayed in a scintillating-fiber target. Fig. 2 shows a diagram of the apparatus. Measurements of charged decay products were made using the target, a central drift chamber, and a cylindrical range stack (RS) composed of 18 layers of plastic scintillator with two embedded layers of tracking chambers. The RS counters in the first layer (T-counters in Fig. 2) were 0.635-cm thick and 52-cm long; the subsequent RS counters were 1.905-cm thick and 182-cm long. The pion from the $K^+ \rightarrow \pi^+ \gamma \gamma$ decay was identified by observation of the $\pi^+ \rightarrow \mu^+ \rightarrow e^+$ decay sequence in the RS using 500-MHz waveform digitizers based on flash analogue-to-digital converters [14]. Trigger counters surrounding the target (I-counters in Fig. 2 which were 0.64-cm thick) and the T-counters surrounding the drift chamber defined the fiducial region. Counters (0.95-cm thick) surrounding the RS helped to suppress the muons from $K^+ \rightarrow \mu^+ \nu$ and $K^+ \rightarrow \mu^+ \nu \gamma$ decays by identifying long-range muons that had completely traversed the RS. A hermetic calorimeter system surrounded the central region. The photons from $K^+ \rightarrow \pi^+ \gamma \gamma$ were detected in a lead/scintillator sandwich barrel detector (BV) surrounding the RS, while two endcap calorimeters and other subsystems (collar, “UPV”, “AD”, and “DPV” in Fig. 2) were used for detecting extra particles. A solenoid surrounding the BV provided a 1 T magnetic field along the beam line.

The AGS proton-beam intensity, and the E949 beam line and apparatus were improved over those used in E787 [15] for the $K^+ \rightarrow \pi^+ \gamma \gamma$ study, which was performed in 1991⁸. The new beam line [16] incorporated two stages of electrostatic particle separation which improved the acceptance for kaons as well as the K^+ to π^+ ratio. The target, central drift chamber, and RS tracking chambers were replaced by a new target consisting of 0.5-cm square fibers, a new low-mass drift chamber [17], and straw-tube chambers, respectively. One third of the RS scintillation counters were replaced to increase the light output. A new photon detector, the barrel veto liner (BVL), was installed to add 2.3 radiation lengths of lead/scintillator sandwich material to the BV. The endcaps were replaced by new fully active detectors consisting of undoped-CsI crystals [18] with significantly increased light output, and both the target and endcaps were read out using 500-MHz waveform digitizers based on charged coupled devices [19] to improve timing and double-pulse resolution. Additional ancillary photon-veto systems [20] and a flasher system of Light Emitting Diode to aid in the RS energy calibration were also introduced.

⁸ Many of the improvements were made in the E787 apparatus after 1991.

The 2002 data set used for this analysis derived from a total exposure of kaons entering the target $N_K = 1.19 \times 10^{12}$. The trigger required a kaon at rest in the target to decay at least 1.5 ns later into a positively charged particle which subsequently came to rest in the RS, accompanied by coincident electromagnetic showers in both the BVL and BV, and no extra energy in the endcap or RS counters. The decay particle was required to penetrate the RS to at least the 16th layer to suppress backgrounds from the monochromatic $K^+ \rightarrow \pi^+\pi^0$ decay ($K_{\pi 2}$) with $P=205$ MeV/c, and no further than the 17th layer to suppress decays into muons. In the RS counter where the particle came to rest, called the “stopping counter”, a $\pi^+ \rightarrow \mu^+$ decay was identified online based on the pulse shape information from the waveform digitizers on the RS. An improved trigger system [21] including a programmable trigger board reduced the online dead time. A total of 1.1×10^7 events met the trigger requirements.

The momentum, equivalent range in plastic scintillator (R), and kinetic energy (E) of the charged track were reconstructed with information from the target, drift chamber and RS. Tracks were accepted for the region defined by $213 \text{ MeV}/c < P < 234 \text{ MeV}/c$, $33.5 \text{ cm} < R < 41.3 \text{ cm}$, and $116 \text{ MeV} < E < 135 \text{ MeV}$, where the lower limits corresponded to 3.3, 2.3, and 2.6 standard deviations, respectively, above the $K_{\pi 2}$ peak ($P = 205 \text{ MeV}/c$, $R = 30.4 \text{ cm}$, and $E = 108 \text{ MeV}$). The larger search region ($P > 213 \text{ MeV}/c$) compared with E787 ($P > 215 \text{ MeV}/c$) resulted from improved kinematic reconstruction, which also removed the requirement of a constrained fit for consistency with $K^+ \rightarrow \pi^+\gamma\gamma$ kinematics that was used in E787 [2].

The timing and energy (E_γ) of the photons were determined by grouping adjacent hit modules in the BVL and BV to classify isolated photon showers (“clusters”). The hit position in each module along the beam axis (z) was calculated from the end-to-end time and energy differences; the azimuthal angle (ϕ) of the hit position in the end view of the detector was determined by the segmentation of the modules. The location of the photon shower in z and ϕ was obtained by an energy-weighted average of the hit positions and was used, in conjunction with the kaon-decay vertex position in the target, to determine the polar and azimuthal angles of the photon as well as the opening angles between the photon and the charged track in the side view ($\theta_{\pi+\gamma}$) and in the end view ($\phi_{\pi+\gamma}$). In approximately half of the $K^+ \rightarrow \pi^+\gamma\gamma$ decays the two photons were unresolved and appear as a single cluster in the BVL and BV, since the opening angle between two photons from $K^+ \rightarrow \pi^+\gamma\gamma$ gets smaller for the events with π^+ momentum close to the kinematic end point. The events with either one or two clusters were accepted; at least one cluster with $50 \text{ MeV} < E_\gamma < 320 \text{ MeV}$, $\theta_{\pi+\gamma} > 155^\circ$, and $\phi_{\pi+\gamma} > 155^\circ$ was required. For events with two clusters, the lower-energy cluster had to have $E_\gamma > 10 \text{ MeV}$.

Background sources from kaon decays at rest were classified into three types:

“*mismeasured*” : $K_{\pi 2}$ decays with mismeasurements of the π^+ and the two photons,
“*overlap*” : $K_{\pi 2}$ decays with the lower-energy photon overlapping the π^+ track in the RS, causing the kinetic energy of reconstructed π^+ track to be incorrectly measured, and
“*muon*” : K^+ decays with a μ^+ misidentified as a π^+ and with photons in the final state (e.g. $K^+ \rightarrow \mu^+ \nu \gamma$, $K^+ \rightarrow \pi^0 \mu^+ \nu$ and $K_{\pi 2}$ with π^+ decay in flight).

Another background source was due to kaon decay in flight:

“*DIF*” : $K_{\pi 2}$ decay-in-flight before the kaon came to rest in the target.

Beam-related backgrounds (e.g. multiple beam particles scattering into the detector) were found to negligible.

These backgrounds were studied from the data by imposing offline selection criteria (“cuts”). The requirements on the π^+ momentum, range and kinetic energy provided large suppression of all of the backgrounds from kaon decays at rest. Several cuts, referred to as “ γ selection cuts”, were imposed to suppress the *mismeasured* background. These included cuts on the following quantities:

- the cut on the invariant mass of two photons to reject events with two clusters and $m_{\gamma\gamma} > 100 \text{ MeV}/c^2$,
- the cut on additional coincident energy to reject events with activity not associated with the π^+ and the candidate signal photons⁹, and
- the cut on the photon clusters to reject events with two photons from a π^0 which hit the same or adjacent modules in BVL and BV and form a single cluster¹⁰ [22].

In addition, only those events whose total photon-shower energy was deposited in the BVL and BV calorimeters were accepted. Cuts on dE/dx in the RS to reject events with a RS counter in which the measured energy was larger than expected from the reconstructed range in that counter were imposed to suppress the *overlap* background [22]. The cuts on the relation between the range measured in the RS and the momentum measured in the drift chamber as well as the cuts on the $\pi^+ \rightarrow \mu^+ \rightarrow e^+$ decay sequence, recorded in the RS stopping counter, were also imposed to suppress the *muon* background. The

⁹ The extra activity was identified in the various subsystems, including the RS, as hits in the counters in coincidence with the π^+ track within a few ns and with energy above a threshold of typically 1 MeV.

¹⁰ Due to the kinematics of $K_{\pi 2}$ and subsequent $\pi^0 \rightarrow \gamma\gamma$ decays, the two photons must hit the modules at different z positions along the beam axis. An event was rejected if the maximum discrepancy among the z -position measurements in the modules of the cluster was larger than 113 cm.

DIF background was suppressed by requiring a delay of at least 2 ns between the time of the kaon coming to rest in the target and its subsequent decay, and by imposing the cuts on the timing between the π^+ in the RS and the K^+ in the Čerenkov counter.

To study and measure these backgrounds, two independent sets of cuts were established for each background source. At least one of these cuts was inverted to enhance each background collected by the $K^+ \rightarrow \pi^+ \gamma \gamma$ trigger as well as to prevent candidate events from being examined before the background studies were completed. To avoid contamination from other background sources, all the cuts except for those being studied were imposed on the data. Possibilities of a correlation between the two sets of cuts or of a biased estimate of the effectiveness of the cuts were studied, and were found to be negligible. The signal acceptance and background levels were studied as a function of cut severity. A comparison of the observed background levels near but outside the signal region was made to the predicted background in these regions. All of these studies [23] were performed in the same manner as the $K^+ \rightarrow \pi^+ \nu \bar{\nu}$ analyses of E787 [24] and E949 [13]. Table 1 summarizes the background levels measured with the final analysis cuts and the two sets of cuts for studying each background source. In total, 0.197 ± 0.070 background events were expected in the signal region.

The acceptance (A) and the single event sensitivity (SES) for $K^+ \rightarrow \pi^+ \gamma \gamma$ in the kinematic region $P > 213$ MeV/ c were derived from the acceptance factors in Table 2 and the total kaon exposure $N_K = 1.19 \times 10^{12}$ times the K^+ -stopping efficiency, which is the fraction of kaons entering the target that came to rest before decaying. The efficiency was measured to be 0.754 ± 0.024 with the $K_{\pi 2}$ events collected by the $K^+ \rightarrow \pi^+ \gamma \gamma$ trigger. We obtained $A = (2.99 \pm 0.07) \times 10^{-4}$ and $SES = (3.72 \pm 0.14) \times 10^{-9}$ for $\hat{c} = 1.8$ including unitarity corrections and $A = (1.10 \pm 0.04) \times 10^{-4}$ and $SES = (1.01 \pm 0.05) \times 10^{-8}$ for $\hat{c} = 1.6$ without the corrections. The former sensitivity was below the predicted branching ratio of 6.10×10^{-9} , giving an expectation of 1.6 events. In order to verify that the sensitivity estimations were correct, a sample of $K^+ \rightarrow \mu^+ \nu$ decays accumulated with a calibration trigger was analyzed. The measured branching ratio of 0.628 ± 0.020 was consistent with the Particle Data Group value [7].

After imposing all analysis cuts, no events were observed in the signal region (Fig. 3). The group of 74 events around $R = 32$ cm and $E = 110$ MeV are due to the $K_{\pi 2}$ background. Taking 2.24 events instead of zero according to the unified approach [25] with the background contribution of 0.197 events, we set a 90% C.L. upper limit on the partial branching ratio $B(K^+ \rightarrow \pi^+ \gamma \gamma, P > 213 \text{ MeV}/c)$ as 8.3×10^{-9} for $\hat{c} = 1.8$ including unitarity corrections and 2.3×10^{-8} for $\hat{c} = 1.6$ without the corrections. The systematic uncertainty was not taken into consideration in deriving the limits. For the purpose of

comparison with the previous E787 results, a 90% C.L. upper limit for the total $K^+ \rightarrow \pi^+ \gamma \gamma$ branching ratio assuming the phase-space distribution was calculated; the present limit 6.0×10^{-8} is 8.3 times lower than the same limit in E787 (5.0×10^{-7}).

The data described above were also used to set an upper limit on the branching ratio for $K^+ \rightarrow \pi^+ \gamma$ decay, which is forbidden by angular-momentum conservation and gauge invariance, but is allowed in noncommutative theories [26]. The signature of $K^+ \rightarrow \pi^+ \gamma$ was a two-body decay of a kaon at rest with a 227-MeV/ c π^+ track in the RS and a 227-MeV photon emitted directly opposite to it and observed in the BVL and BV calorimeters. The trigger, event reconstruction, and offline selection criteria in the study of $K^+ \rightarrow \pi^+ \gamma \gamma$ had been designed so that the same data were available to the search for $K^+ \rightarrow \pi^+ \gamma$. Since the background levels were already small, the π^+ accepted region was not reduced for the $K^+ \rightarrow \pi^+ \gamma$ analysis. The previous limit from the E787 study was 3.6×10^{-7} [22] (90% C.L.) from data collected in 1996–1997 with a highly prescaled trigger with relaxed trigger-conditions resulting in the total kaon exposure of 6.7×10^8 . The new 90% C.L. upper limit from E949, using the acceptance for $K^+ \rightarrow \pi^+ \gamma$ of $(1.08 \pm 0.02) \times 10^{-3}$, is 2.3×10^{-9} .

The results from this study cannot confirm nor rule out the unitarity corrections of ChPT, but the upper limits obtained are the most restrictive yet achieved on $K^+ \rightarrow \pi^+ \gamma \gamma$ and as well as on $K^+ \rightarrow \pi^+ \gamma$. The E949 experiment has been shown to be suitable for the study of $K^+ \rightarrow \pi^+ \gamma \gamma$ in the π^+ momentum region close to the end point. The experimental uncertainty is limited by statistics; additional data is required to more stringently test the predictions of ChPT for this decay. The possibility to observe the $K^+ \rightarrow \pi^+ \gamma \gamma$ decay in the kinematic region, if the ChPT including unitarity corrections is correct, gives further impetus for additional data collection.

Acknowledgements

We gratefully acknowledge the dedicated effort of the technical staff supporting E949 and of the Brookhaven C-A Department. We are also grateful to G. D'Ambrosio, F. Gabbiani, G. Isidori, and G. Valencia for useful discussions. This research was supported in part by the U.S. Department of Energy, the Ministry of Education, Culture, Sports, Science and Technology of Japan through the Japan-U.S. Cooperative Research Program in High Energy Physics and under Grant-in-Aids for Scientific Research, the Natural Sciences and Engineering Research Council and the National Research Council of Canada, the Russian Federation State Scientific Center Institute for High Energy Physics, and the Ministry of Science and Education of the Russian Federation.

References

- [1] B. Bassalleck *et al.*, E949 Proposal, BNL-67247, TRI-PP-00-06 (1999), [<http://www.phy.bnl.gov/e949/>] .
- [2] P. Kitching *et al.*, Phys. Rev. Lett. 79 (1997) 4079.
- [3] A.J. Buras, F. Schwab, and S. Uhlig, hep-ph/0405132, and references therein.
- [4] J.F. Donoghue, E. Golowich, and B.R. Holstein, *Dynamics of the Standard Model* (Cambridge University Press, Cambridge, 1992), and references therein.
- [5] G. Ecker, A. Pich, and E. de Rafael, Phys. Lett. B 189 (1987) 363; Nucl. Phys. B 303 (1988) 665; L. Cappiello and G. D'Ambrosio, Nuovo Cimento A 99 (1988) 155.
- [6] G. D'Ambrosio and J. Portolés, Phys. Lett. B 389 (1996) 770; Nucl. Phys. B 492 (1997) 417; Nucl. Phys. B 533 (1998) 494.
- [7] Particle Data Group, S. Eidelman *et al.*, Phys. Lett. B 592 (2004) 1.
- [8] G. Ecker, A. Pich, and E. de Rafael, Phys. Lett. B 237 (1990) 481; L. Cappiello, G. D'Ambrosio, and M. Miragliuolo, Phys. Lett. B 298 (1993) 423; A.G. Cohen, G. Ecker, and A. Pich, Phys. Lett. B 304 (1993) 347.
- [9] A. Alavi-Harati *et al.*, Phys. Rev. Lett. 83 (1999) 917.
- [10] A. Lai *et al.*, Phys. Lett. B 536 (2002) 229.
- [11] F. Gabbiani and G. Valencia, Phys. Rev. D 64 (2001) 094008; Phys. Rev. D 66 (2002) 074006.
- [12] G. Buchalla, G. D'Ambrosio, and G. Isidori, Nucl. Phys. B 672 (2003) 387.
- [13] V.V. Anisimovsky *et al.*, Phys. Rev. Lett. 93 (2004) 031801.
- [14] M.S. Atiya *et al.*, Nucl. Instrum. Methods Phys. Res., Sect. A 279 (1989) 180.
- [15] M.S. Atiya *et al.*, Nucl. Instrum. Methods Phys. Res., Sect. A 321 (1992) 129.
- [16] J. Doornbos *et al.*, Nucl. Instrum. Methods Phys. Res., Sect. A 444 (2000) 546.
- [17] E.W. Blackmore *et al.*, Nucl. Instrum. Methods Phys. Res., Sect. A 404 (1998) 295.
- [18] I-H. Chiang *et al.*, IEEE Trans. Nucl. Sci. 42 (1995) 394; T.K. Komatsubara *et al.*, Nucl. Instrum. Methods Phys. Res., Sect. A 404 (1998) 315.
- [19] D.A. Bryman *et al.*, Nucl. Instrum. Methods Phys. Res., Sect. A 396 (1997) 394.
- [20] O. Mineev *et al.*, Nucl. Instrum. methods Phys. Res., Sect. A 494 (2002) 362.

- [21] T. Yoshioka *et al.*, IEEE Trans. Nucl. Sci. 51 (2004) 334.
- [22] S. Adler *et al.*, Phys. Rev. D 65 (2002) 052009.
- [23] T. Yoshioka, Ph.D. thesis, University of Tokyo, 2005.
- [24] S. Adler *et al.*, Phys. Rev. Lett. 88 (2002) 041803; S. Adler *et al.*, Phys. Rev. Lett. 84 (2000) 3768; S. Adler *et al.*, Phys. Rev. Lett. 79 (1997) 2204.
- [25] G.J. Feldman and R.D. Cousins, Phys. Rev. D 57 (1998) 3873.
- [26] J. Trampetić, hep-ph/0212309; B. Melic, private communication.

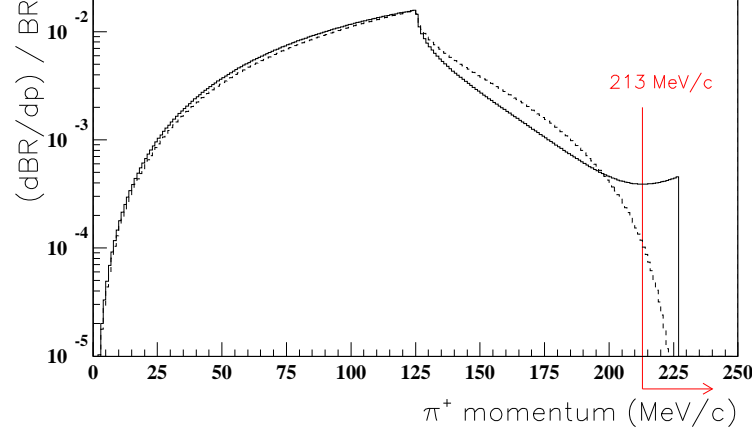


Fig. 1. Predictions for the π^+ momentum for the ChPT parameter $\hat{e} = 1.8$ including unitarity corrections (solid line) and for $\hat{e} = 1.6$ without the corrections (dashed line) as described in the text. The ratios of the partial branching ratio in the kinematic region $P > 213 \text{ MeV}/c$, indicated by the arrow, to the total branching ratio are 5.77×10^{-3} and 0.515×10^{-3} , for $\hat{e} = 1.8$ and $\hat{e} = 1.6$ respectively.

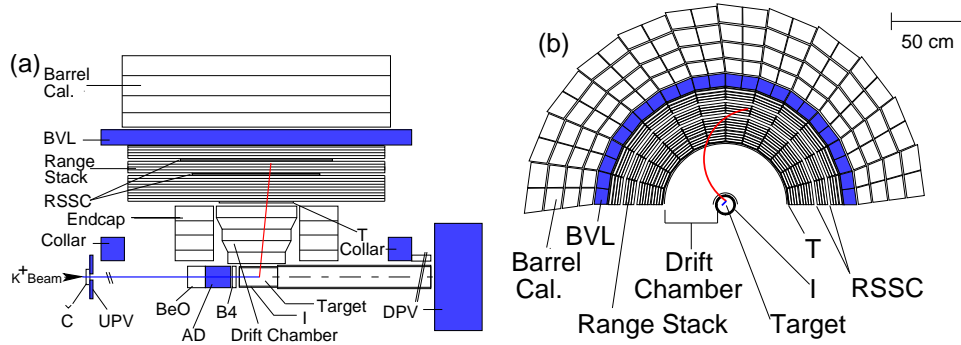


Fig. 2. Schematic side (a) and end (b) views of the upper half of the E949 detector. Č: Čerenkov counter; B4: energy-loss counters; I and T: inner and outer trigger scintillation counters; RSSC: RS straw-tube tracking chambers. New or upgraded subsystems for E949 (shaded) included the barrel veto liner (BVL), collar, upstream photon-veto (UPV), active degrader (AD), and downstream photon-veto (DPV).

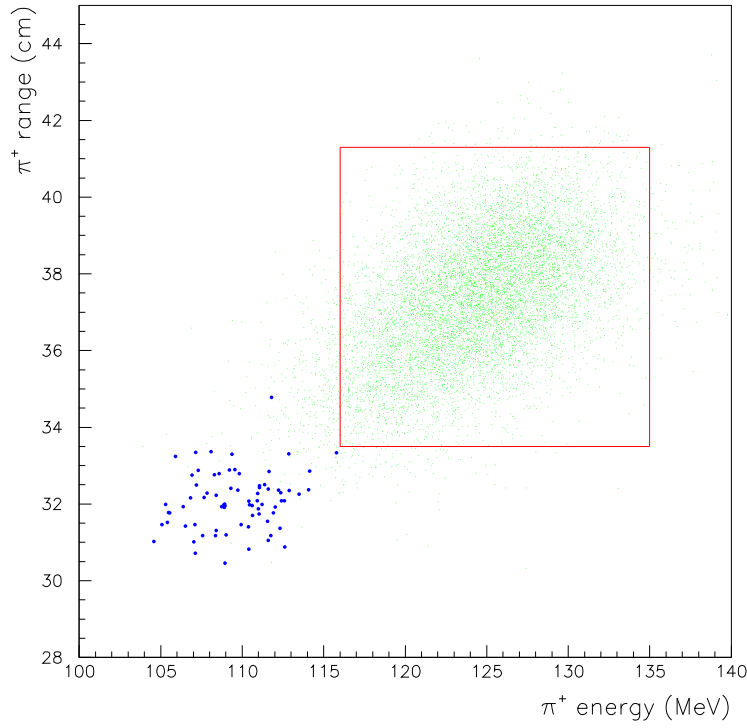


Fig. 3. Range (equivalent cm of plastic scintillator) vs. kinetic energy (MeV) plot of the events with all analysis cuts imposed. The box indicates the signal region for the $K^+ \rightarrow \pi^+ \gamma \gamma$ decay. The dark points represent the data. The simulated distribution of expected events from $K^+ \rightarrow \pi^+ \gamma \gamma$ for $\hat{c} = 1.8$ including unitarity corrections is indicated by the light dots.

Source	background level	two sets of cuts	
<i>mismeasured</i>	0.017 ± 0.006	π^+ accepted region (P,R,E)	γ selection
<i>overlap</i>	0.065 ± 0.065	π^+ accepted region (P,R)	$\pi^+ dE/dx$
<i>muon</i>	0.090 ± 0.020	π^+ accepted region (P,R,E) π^+ range-momentum relation	$\pi^+ \rightarrow \mu^+ \rightarrow e^+$
<i>DIF</i>	0.025 ± 0.014	delay in the target	RS - Č timing

Table 1

Expected background levels in the signal region and the two sets of cuts for studying each background source. The total background was 0.197 ± 0.070 events.

Acceptance factors	UC	w/o UC	samples
Trigger	0.0623	0.0407	MC, K_B
π^+ reconstruction and fiducial cuts	0.980	0.935	MC, $K_{\mu 2}$
π^+ accepted region (P, R, E)	0.912	0.667	MC
π^+ stop without nuclear interaction or decay-in-flight	0.492	0.524	MC
dE/dx and kinematic cuts	0.537	0.537	$K_{\pi 2}$, π_{scat}
$\pi^+ \rightarrow \mu^+ \rightarrow e^+$ cuts	0.349	0.349	π_{scat}
γ reconstruction and fiducial cuts	0.530	0.492	MC, $K_{\pi 2}$
γ selection cuts	0.216	0.177	MC, $K_{\pi 2}$
Other cuts on beam and target	0.507	0.507	$K_{\mu 2}$
Total acceptance	2.99×10^{-4}	1.10×10^{-4}	

Table 2

Acceptance factors for the $K^+ \rightarrow \pi^+ \gamma \gamma$ decay in the kinematic region $P > 213$ MeV/ c , for $\hat{c} = 1.8$ including unitarity corrections (“UC”) and for $\hat{c} = 1.6$ without the corrections (“w/o UC”), and the samples used to determine them. “MC” in the rightmost column means the sample generated by Monte Carlo simulation. “ K_B ”, “ $K_{\mu 2}$ ”, “ $K_{\pi 2}$ ”, and “ π_{scat} ” mean the data samples of kaons entering the target, $K^+ \rightarrow \mu^+ \nu$ decays, $K_{\pi 2}$ decays, and scattered beam pions, respectively; these samples were accumulated by calibration triggers simultaneous to the collection of signal candidates.